Analysis of Patient Responses to CAR T Therapy Using Single-Cell Multiomics Profiling

Je-Won Im

November 2022

Fan Lab
Yale School of Engineering & Applied Sciences

ABSTRACT

Chimeric antigen receptor (CAR) T cell therapy is a rising method of immunotherapy for treating cancer, especially in B cell acute lymphoblastic leukemia (ALL). However, even with the same CAR modifications, patient responses range from complete remission to relapse and no response. Because many negative responses are caused by T cell shortcomings instead of factors in the tumor microenvironment, genetic engineering of the CAR as well as gene enhancement and knockout can improve CAR T efficacy. Single-cell profiling allows a closer look at specialized functions by T cell subtypes instead of generalizing the entire CAR T population. Here, I use single-cell transcriptomic and proteomic data of 59,116 cells from 7 B-ALL patients and 31,032 cells from 4 healthy donors to show the differentially expressed genes (DEGs) between different patient responses. By using DEG and gene ontology enrichment analysis, a subset of no response patient cells were found to have decreased key CAR T functions such as cytotoxic, helper, stimulatory, and cytokine activities. These cells had elevated Treg pathways, showing higher susceptibility to apoptosis but proliferating greater than other T cell subtypes in the short-term, thus decreasing the long-term duration of CAR T and likely contributing to the lack of therapeutic response *in vivo*. These findings further our understanding of CAR T cell subtypes and could provide a way on modifying genes and pathways of T cells to improve upon CAR T efficacy and persistence in B-ALL, as well as shedding light on applications to other types of cancer.

INTRODUCTION

Adoptive T cell transfer (ACT) is the use of lymphocytes to combat tumors and reduce the effects of rejection from organ allografts (Billingham *et al.* 1954, Mitchinson 1955). One emerging type of ACT developed for cancer therapy is chimeric antigen receptor (CAR) T cells, which uses the substitution of a single-chain variable fragment (scFv) with a TCRς chain from the regular double-chain T cell receptors (TCRs) (Zhang *et al.* 2017, June and Sadelain 2018). While TCRs have an antigen-specific response based on their variable antigen-binding site, the scFv of all CAR T cells target the same set of tumor-specific proteins, and the single chain facilitates genetic engineering and modifications.

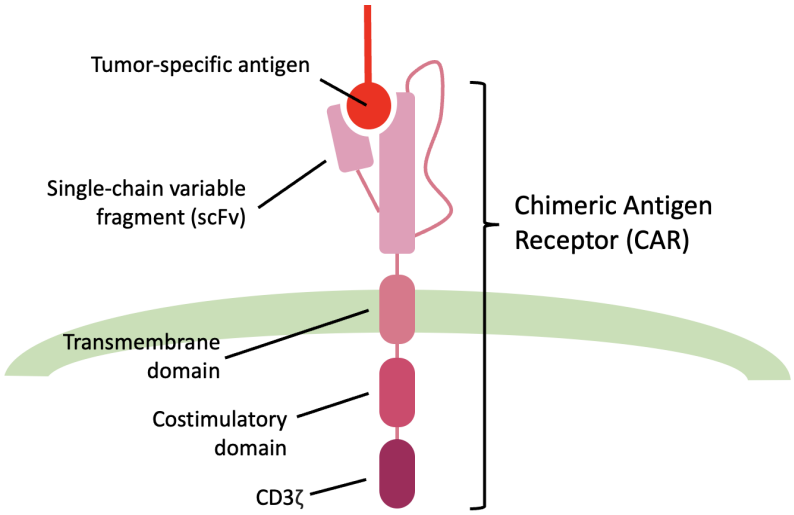

Figure 1: Design of a Chimeric Antigen Receptor (CAR).
The scFv that binds to the tumor-specific antigen replaces the antigen-binding site of a regular TCR consisting of alpha and beta chains. Into the membrane, several costimulatory domains such as CD28 can be added to accurately target tumor cells (Figure adapted from June and Sadelain 2018).

An ACT that uses TCR engineering instead of CAR recognizes molecules bound to the MHC of antigen-presenting cells or tumors; however, this method is known to target the body's own cells, and cannot avoid toxicity while still having effective clinical treatment (He *et al.* 2019, Dhatchinamoorthy *et al.* 2021, Wang and Cao 2020). CAR T therapy is effective because it does not target tumors through the major histocompatibility complex (MHC) of cells, unlike other ACT treatments like TCR, reducing off-tumor targeting (Garrido *et al.* 2016). Once activated, CAR T cells proliferate and activate non-CAR T cells for tumor responses, which overcomes the autoimmunity challenges of cancer treatment (Finn 2008, June *et al.* 2017). Targeting the CD19 surface molecule on tumor cells has been effective in treating

B cell malignancies, especially B cell acute lymphoblastic leukemia (ALL) (Brentjens *et al.* 2013, Grupp *et al.* 2013), due to the unique characteristic of CD19 being only found on cells of the B cell lineage (LeBien and Tedder 2008).

While the recent FDA commercial approvals of CAR T cell therapy show successes and efficacy in treating cancer (Sengsayadeth *et al.* 2021, Le *et al.* 2018, Lin *et al.* 2022), several limitations still pose problems in treating a greater number of patients successfully. There are four main types of issues: first, CAR T cells may not proliferate properly once transferred back into the patient's body, resulting in short-term or no response. Second, tumors show adaptive resistance such as CD19 loss, which is present in up to 28% of acute leukemia cases (June *et al.* 2018). Third, toxicities arise from immunotherapy because of the number of immune cells activated, which can result in severe cytokine release syndrome (CRS) or neurotoxicity (Davila *et al.* 2014, Lee *et al.* 2014, Teachey *et al.* 2016). Last, CAR T therapy is currently limited to targeting cancers of the B cell lineage and cannot target solid tumors, though new cellular engineering with adding co-stimulatory molecules and secondary target molecules has widened the possibilities (June and Sadelain 2018).

Such limitations result in various patient responses, ranging from no response, relapse, and complete remission. CAR T cell therapy, once fully developed, potentially can provide a cheaper alternative to high-cost therapies and even introduce an off-the-shelf treatment for cancer, as scFv engineering stays constant between different T cells (Zakrzewski *et al.* 2008, Torikai *et al.* 2012). By finding the varying pathways that differ between no response patients and complete remission patients, the discovery of cellular functions that will improve the efficacy of CAR T treatment will contribute to the further improvement of genetic engineering in CAR and cellular modification. In this research, I analyze differentially expressed genes (DEGs) and proteins between various patient CAR T cell samples and T cell subtypes within these samples in order to find markers of complete remission and no response patients.

METHODS

Patient samples

Samples of pediatric patients with resistant or refractory B-ALL were collected from two separate trials at the University of Pennsylvania and the Children's Hospital of Pennsylvania. One set of samples were collected from trials aimed to determine the safety and feasibility of CART-19 cell therapy and the proliferation and duration in vivo (ClinicalTrials.gov, NCT01626495). Another set of samples were

obtained from a pilot trial on the effect of tocilizumab on the risk of CART-19 associated cytokine release syndrome (ClinicalTrials.gov, NCT02906371). All laboratory operations involving the collection and analysis of samples followed the International Conference on Harmonization Guidelines for Good Clinical Practice, and ethical standards were ensured.

Single-cell multiomics profiling

Protocols follow those described in Bai *et al.* 2022. Patient T cell samples were transduced using a lentiviral vector containing a CD19-specific CAR with 4-1BB/CD3 transgene. An *in vitro* coculture assay was created through the NIH3T3 mouse fibroblast line. The CD19 environment was NIH3T3 cells transduced with human CD19 (CD19-3T3), and the negative control expressed mesothelin (MSLN-3T3). CTL019 cells were cocultured in the CD19-3T3 and MSLN-3T3 cells to produce stimulated and control samples. CAR+ cells were stained for CITE-seq, prepared for scRNA-seq, then sequenced. A unique molecular identifier (UMI) count matrix filtered mouse cells and low-quality mRNAs from the sequenced data.

Differentially expressed gene (DEG) analysis

The Seurat v4.0 software was used to perform integration, QC, and differential expression analysis of the multimodal CITE-seq data from Bai *et al.* 2022. The integration of different samples followed the standard Seurat workflow using anchor points and canonical correlation analysis (CCA) (Stuart *et al.* 2019). To reduce the memory usage, reverse PCA was done beforehand, and the integration using the SCTransform function involved the first 30 dimensions. Default numbers were used for CCA dimensions and anchor neighbors. QC was performed with a lower and upper bound for mRNA expression and the fraction of mitochondrial genome. The ADT assay was normalized, and the integrated data were visualized in two dimensions using UMAP. Top markers for each cluster were found using the FindMarkers function.

GO enrichment analysis

The ShinyGO 0.76 gene enrichment analysis tool (http://bioinformatics.sdstate.edu/go/) was used in determining GO terms and enriched pathways. Top markers for various states were exported from Seurat FindMarkers and entered into ShinyGo to produce a fold enrichment lollipop chart.

High Performance Computing Clusters

The Yale University High Performance Computing (HPC) clusters were used to accommodate for the high memory usage of the integration and analysis. The general partition from the Ruddle cluster of the Yale Center for Genome Analysis was used to store patient data and run analysis through interactive RStudio Server. With memory reduction algorithms, the environment required approximately 100 to 115 gigabytes along with a single node and core.

RESULTS

The data analysis was performed in three phases: an analysis of the 4 healthy donor samples, the 7 patient samples, and a fully integrated dataset of both healthy donors and patients.

Healthy donor data shows divergence of stimulated and basal state cells through UMAP clustering

The dataset of the healthy donors' single-cell multiomics profile, consisting of 31032 cells with 36601 RNA features, was first filtered through quality control (QC) to remove low-quality cells, empty droplets, or doublets and multiplets from the scRNA-seq protocol. Low-quality data from these cells may affect analysis due to artificially high or low gene expression. Lower and upper bounds on the number of features, total count of the RNA expression, and percentage of mitochondrial genome for the filtered cells was determined through a violin plot visualization (Figure 1). Cells with 200 to 5000 unique features and a mitochondrial genome percentage below 10% were selected for analysis, resulting in 25896 cells, with 5136 cells being filtered.

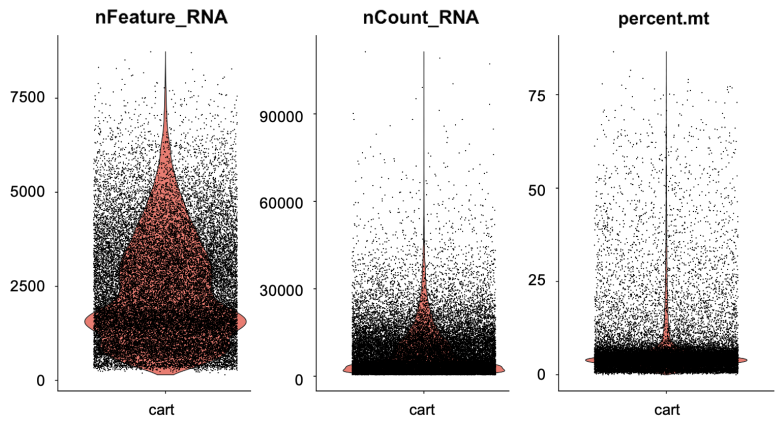

Figure 1: Violin plots in determining Quality Control (QC) of the healthy donor dataset (n=31032).
Left: the number of unique features (RNA) found in each cell.
Middle: the total number of RNA counts from each cell, generally correlating with the number of features.
Right: The percentage of mitochondrial genome comprising the feature count.

The filtered dataset was then visualized after log normalization and scaling, which initially yielded 15 clusters total. Because there are a limited number of T cell subsets that can be identified, different resolutions were tried out to yield an optimal number of clusters, with res=0.4 creating 11 clusters.

To show the differences between basal state (BA) and stimulated (CD) cell conditions from the overall UMAP clustering, the dataset was divided into their sub states based on their hashtag oligonucleotide (HTO) identification. The proteomic data consisted of two types of proteins: antigen-derived tags (ADTs) recording the expression of the cell surface protein levels and hashtag oligonucleotides (HTOs) identifying the sample type of the cells. ADT and HTO expression data were normalized through centered log-ratio transformation. Through HTO demultiplexing, cells could be separated based on their HTO index. From the 4 healthy donors, HTO indices 1-4 corresponded to CD cells and indices 5-8 to BA cells (Figure 2). Highlighting each sample type on the overall UMAP showed that the difference between stimulated and basal states was much greater than the difference between individual donors (Figure 3). Clusters 1 and 10 contain a mostly even mix of all 8 samples, indicating that it was a common subset of all CAR T cells. Basal state cells were most prominent in clusters 0, 3, and 7, and stimulated cells were in clusters 2, 4, 5, 6, 8, and 9, suggesting that CAR T cells divided into more diverse and distinct functions once in presence of the target CD19 proteins.

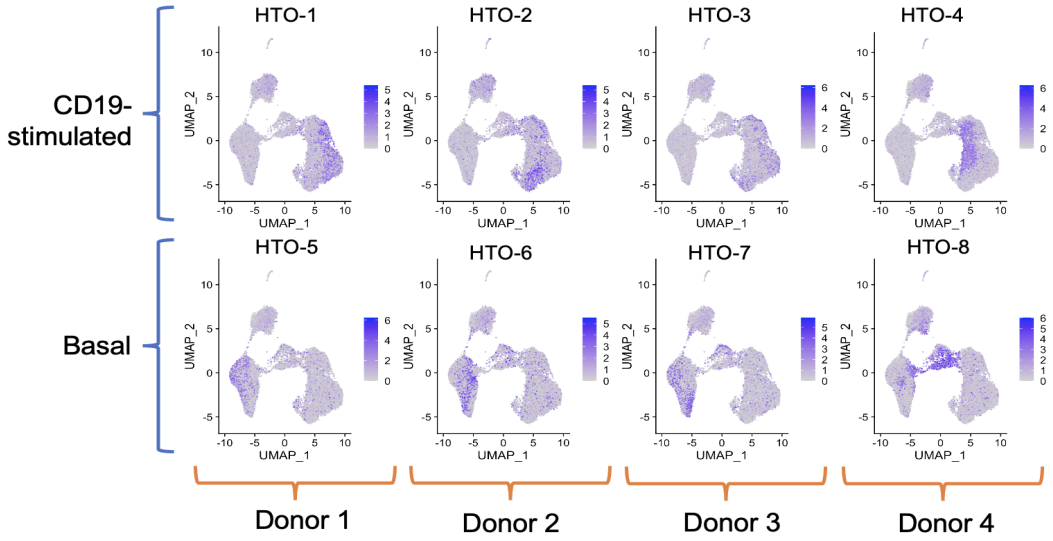

Figure 2: Structure of the HD dataset through HTO demultiplexing, each highlighted as locations on the overall UMAP.

HTO-1 through HTO-4 were cells co-cultured with CD19-expressing 3T3 cells, while HTO-5 through HTO-8 were cells co-cultured with mesothelin-expressing 3T3 cells. HTO-1 and HTO-5 were from the same donor, HTO-2 and HTO-6 from a second donor, HTO-3 and HTO-7 from a third, and HTO-4 and HTO-8 from a fourth, for 4 donors in total.

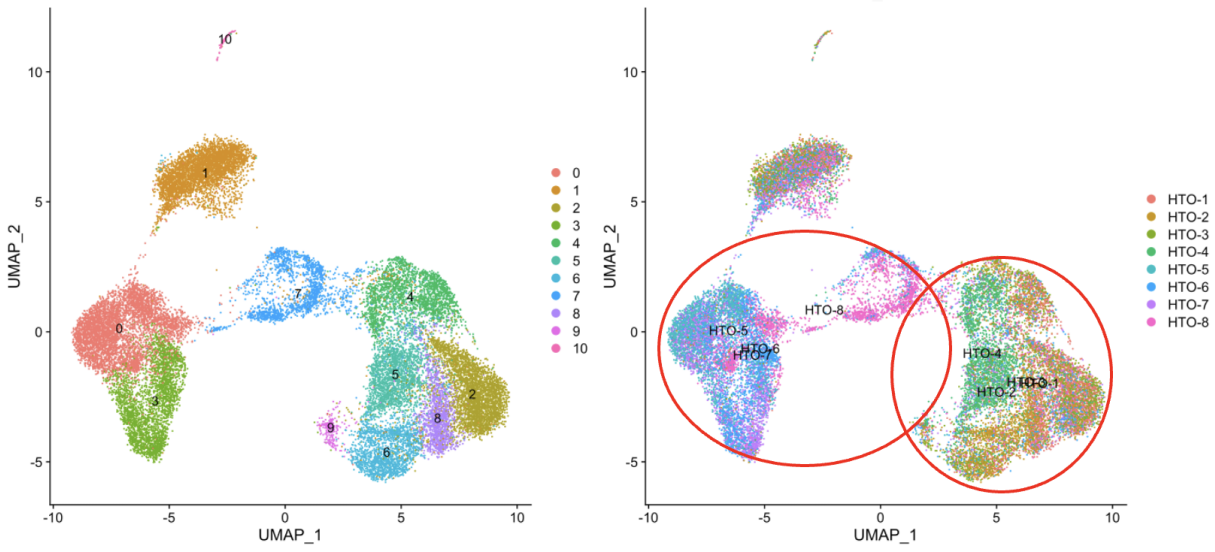

Figure 3: Localization of stimulated and basal-state donor samples onto the overall clustering.

Left: original UMAP visualization, with 11 clusters.

Right: HTO tags mapped onto the same clustering, with HTO-5 through HTO-8 mainly on the left side of the UMAP, and HTO-1 through HTO-4 on the right, and clusters 1 and 10 being a mix of every donor.

HTO demultiplexing of healthy donor data reveals activation and regulation of key protein and transcriptional markers

HTO demultiplexing revealed important insights into ADT and RNA expression analysis by showing differential expression of genes and proteins between the two stimulation states. Of the 17 cell surface proteins whose levels were recorded, 3 showed prominent differences between stimulated and basal conditions (Figure 4a). CD69 and LAG-3 were expressed highly in stimulated cells, and CD62L was expressed highly in basal state cells. The CD4 and CD8 proteins, markers for helper and cytotoxic T cells respectively, showed similar counts across both stimulation states and individual donors (Figure 4b).

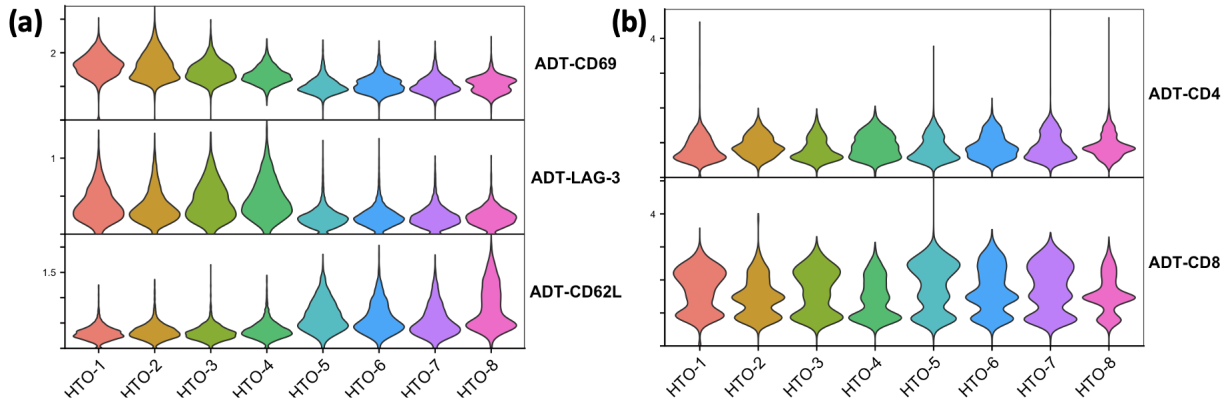

Figure 4: Differential expression of notable ADT markers between stimulated and basal state cells.
(a) Expression levels of CD69, LAG-3, and CD62L by each HTO tag. CD69 and LAG-3 are more highly expressed in HTO-1 through HTO-4, and CD62L is more highly expressed in HTO-5 through HTO-8.
(b) Expression levels of CD4 and CD8 by HTO index.

Key immunological markers of T cell subtypes were also shown to differ between stimulated and basal state cells (Figure 5a). Overall, stimulated cells had higher cytotoxic and helper activity, as seen most prominently in the granzyme gene *GZMB* and T cell type 1 helper (Th1) markers *IFNG* and *IL13*. In stimulatory features, *CSF2* showed a notably higher expression in stimulated cells (Figure 5b), despite some previous literature observing that CAR T activation could be independent of CSF2 expression (Bai *et al.* 2021). On the other hand, basal state cells had generally higher regulatory activities, especially with the feature *TGFB1*. Chemokine activity varied between states, with *CCL3*, *XCL1*, and *XCL2* levels higher on stimulated cells, *CCL5* higher on basal state cells, and *CC4*, *CXCL10*, and *CCL20* similarly expressed across all donors.

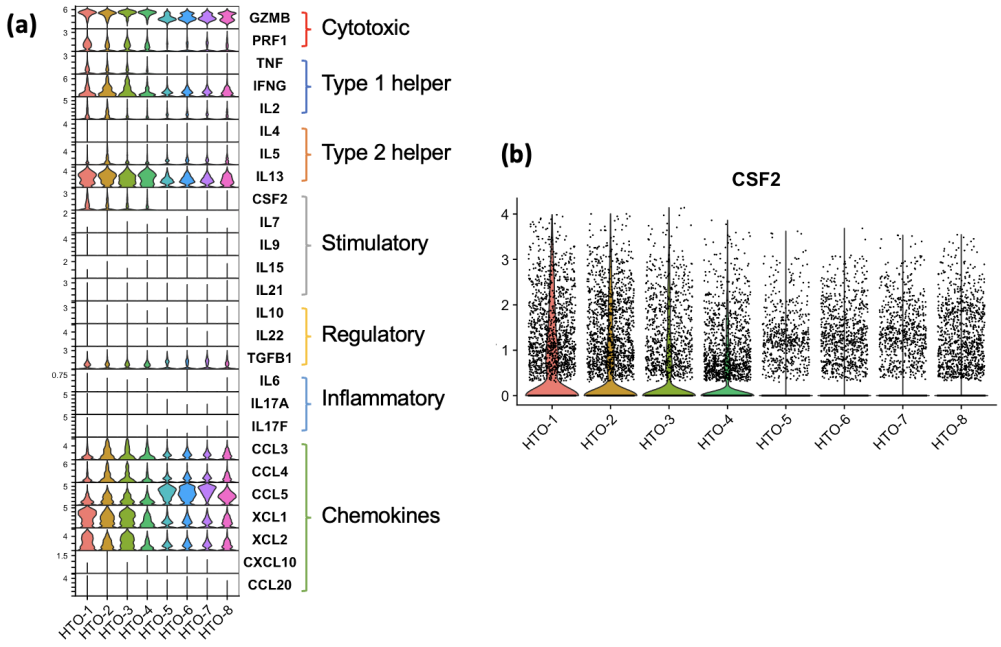

Figure 5: Key immunological genes from literature defining specific subtypes of T cells.

(a) The expression levels of each sample, by HTO index, are graphed in a stacked violin plot. The different subtypes of T cells shown are cytotoxic, type 1 and 2 helpers, stimulatory, regulatory, inflammatory, and chemokine-related T cells.

(b) Detailed view of *CSF2* expression from (a).

GO analysis of complete remission and no response patient data show distinct clustering corresponding to subtypes of CAR T cells with differing functions and pathways

The activation and regulatory markers expressed under healthy conditions would uncover differences in CAR T activation between complete remission (CR) and no response (NR) patients. In total, stimulated and basal state samples from 7 patients, consisting of 4 CR patients and 3 NR patients, were used in the patient response analysis. 70305 cells were integrated, and cells with less than 300 features, more than 6000 features, or a percent mitochondrial genome greater than 10% were filtered, leaving a subset of 59116 cells after QC. When separated into further subsets, UMAP clustering showed a greater divergence between stimulated conditions (CD vs BA) than compared to patient responses (CR vs NR) (Figure 6). Stimulated cells were concentrated in clusters 1 and 10, while basal state cells were most present in clusters 0 and 4 (Figure 6b). On the other hand, the two types of patient cells were more evenly distributed throughout most clusters, with the exception of cluster 10 with a high proportion of NR cells (Figure 6c).

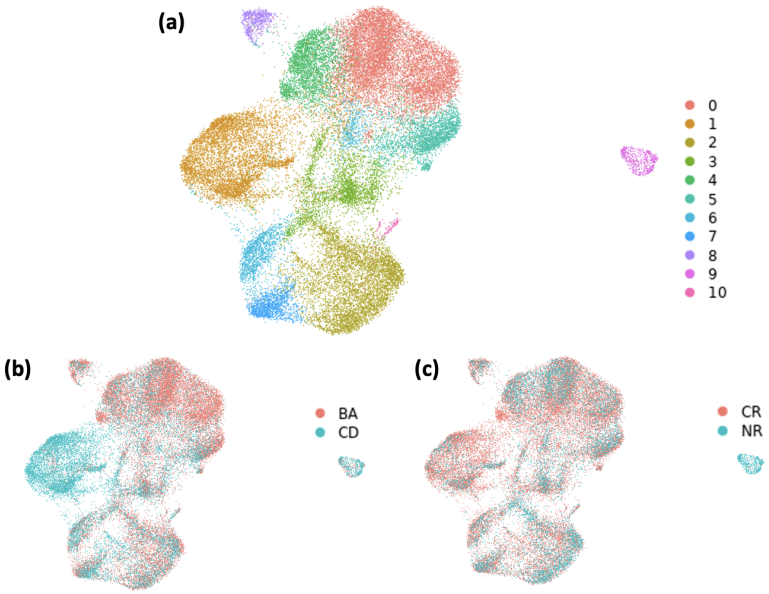

Figure 6: UMAP plot of the patient dataset highlighted in various forms.

(a) Original clustering showing 11 different clusters.

(b) Basal (BA) and stimulated (CD) cells highlighted onto the UMAP.

(c) Complete remission (CR) and no response (NR) patient cells highlighted.

Clustering separately by CD and BA states provided a greater insight into the molecular pathways of subtypes of the CAR T cell population. The stimulated subset yielded 10 clusters, while the basal state yielded 12 (Figure 7ab). Upon GO analysis, the stimulated subset clusters 1 and 2, the clusters with the greatest CR/HD proportion, had high expression of common CAR T pathways involving immune cell differentiation and activation (Figure 7c). CD cluster 8, with a >90% NR proportion, showed regular biological and non-CAR T specific pathways involving protein targeting, localization, and endoplasmic reticulum-related activities (Figure 7d). BA clusters 8 and 10 with also the greatest CR/HD proportion showed similarity to CD clusters 1 and 2, with cluster 8 expressing pathways in apoptotic signaling and cell death, and cluster 10 in immune cell differentiation and activation. BA cluster 11 was similar to CD cluster 8, with protein targeting, localization, and ER-related pathways, indicating that this subset of NR cells kept the same functions upon stimulation.

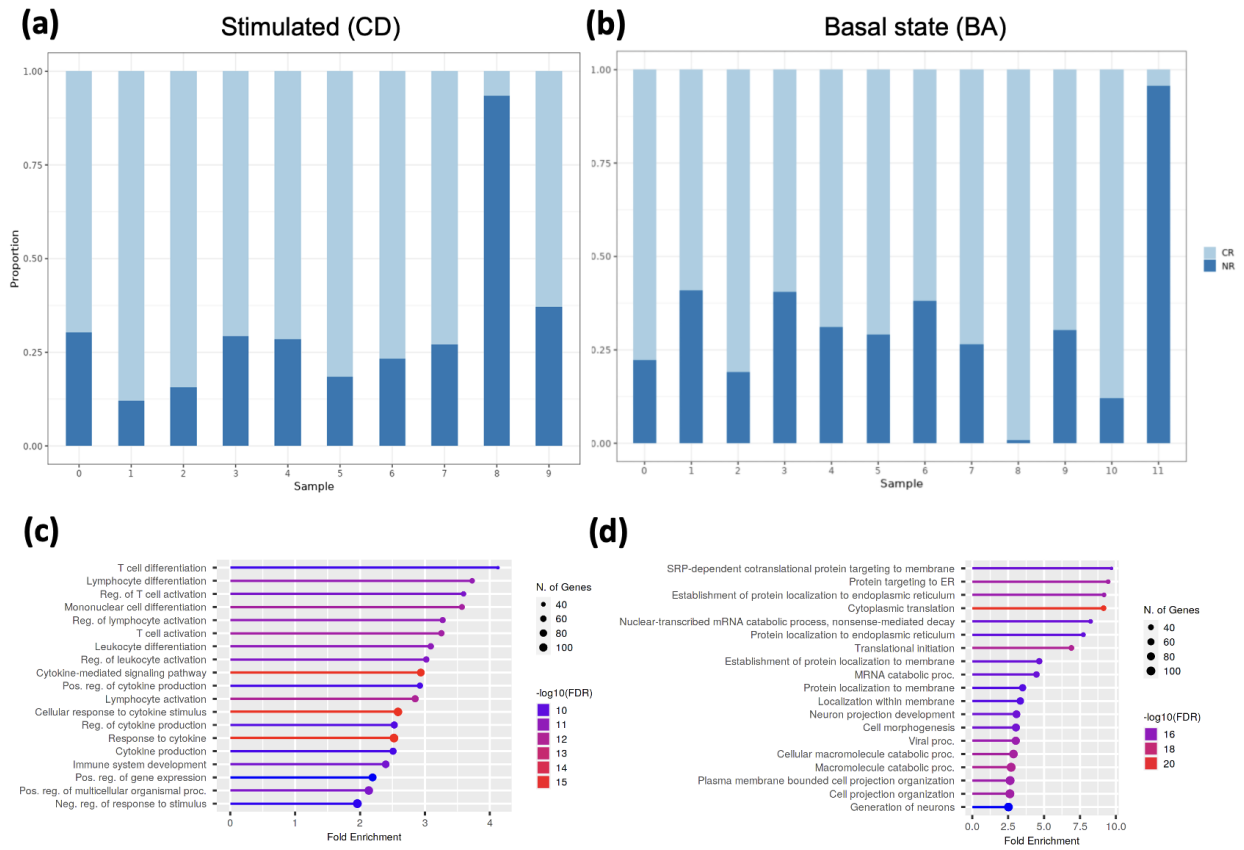

Figure 7: Cluster analysis of patient data after separation of stimulation states.

(a) Proportion of patient response types in the 10 clusters (0-10, res=0.3) of CD cells. CR cells (light blue) dominate NR cells (navy) in all clusters but cluster 8.

(b) Proportion of patient response types in the 12 clusters (0-12, res=0.3) of BA cells. NR dominates cluster 11.

(c) GO analysis showing pathways of cluster 1 of the CD subset, most notably showing T cell differentiation, activation, and production and response to cytokines and stimulus.

(d) GO analysis showing pathways of cluster 8 of the CD subset, showing protein localization, targeting to the ER, and cell projection organization. Pathways such as viral processes and generation of neurons can be disregarded due to the limitations of the GO enrichment analysis software.

Integration of healthy donor and patient data increases sample size and reveals differential expression in key immunological genes and pathways

To further analyze the markers distinguishing CR and NR patient response, the healthy donor data was integrated into the patient dataset. Because HD features showed similar expression to CR patients, this was done to make the sample size larger. The UMAP showed less divergent clustering than UMAPs from the HD or patient data each, with 13 clusters total (Figure 8a). Analysis of the proportions of CR, HD, and

NR samples in each cluster showed that cluster 3 had the lowest NR percentage and 12 the highest, which corresponded to the UMAP visualization of clusters 3 and 12 diverging the most from the rest of the clusters (Figure 8b).

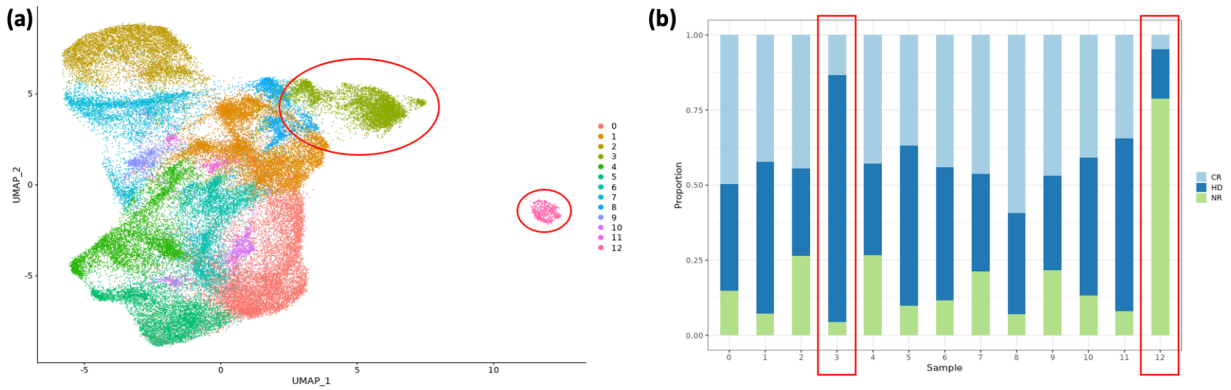

Figure 8: UMAP of integrated data and proportions of CR/HD/NR cells in the clustering (n=85012).
(a) 13 clusters of the fully integrated dataset, with 50 dimensions of reverse PCA performed before the integration, then using 30 dimensions for the final projection. Clusters 3 and 12 are circled in red.
(b) Proportions of the CR (light blue), HD (navy), and NR (green) cells within the 13 unsupervised clusters. Clusters 3 and 12 are boxed in red, corresponding to the circles in (a).

Dividing the dataset into basal state and stimulated conditions yielded 12 and 13 clusters, respectively (Figure 9). BA clusters 7 and 11 were majority CR-based; cluster 7's pathways included T cell, leukocyte, and lymphocyte activation, as well as cell cycle activities. BA cluster 11 showed high expression of cell migration, locomotion, differentiation, and development pathways. BA cluster 12 was mostly NR and, similar to the patient data, showed activities in protein targeting, localization, and ER-related pathways. In the CD subset, cluster 10 was analogous to BA cluster 12, with having a majority NR proportion and showing regular biological activities not related to CAR T functions; it also had pathways related to the mRNA catabolic production.

Most other clusters in the CD subset had very low percentages of NR and high CR and HD cells. There were several defining characteristics of each of these clusters. Clusters 0 and 3 were both related to lymphocyte activation; cluster 0 specifically had high levels of cytokine regulation and the negative regulation of apoptosis. Cluster 5 also showed high cytokine production and proliferation activities. Clusters 3, 6, and 9 were all related to cell-cell adhesion, which is a necessary step in immune cell activation by CAR T cells. Cluster 6 was shown to mainly target CD4+ T helper cells. Finally, clusters 1

and 11 were related to pathways in mitosis, cell division, and the cell cycle, indicating proliferation; cluster 11 also had negative regulation of transcriptional activities.

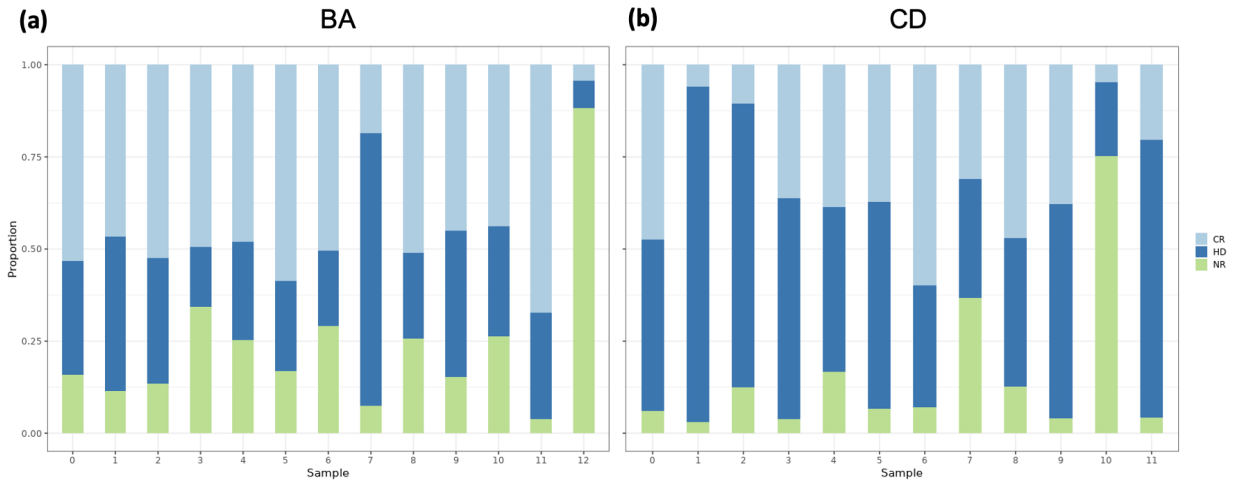

Figure 9: Proportions of CR (light blue), HD (navy), and NR (green) cells within the clustering of BA and CD cells.

Analogous to Figure 7, but with the fully integrated dataset instead of solely from the patient data. BA cluster 12 shows the highest NR cell proportion, similar to CD cluster 10. CD cells show a high percentage of HD cells overall.

(a) Basal state cell subset, with 13 clusters total.

(b) Stimulated cell subset, with 12 clusters total.

Specific key immunological gene markers, in addition to these overarching cellular pathways, were analyzed through the unsupervised clusters (Figure 10). In BA cells, cluster 7 showed the highest cytokine production—aligning with the previous finding of a high proportion of CR cells in BA cluster 7. In stimulated cells, cluster 3 showed the highest cytokine production, especially with chemokines such as CCL3 and CCL4. CD cluster 10 notably showed a lack of overall cytokine production, also in line with the high proportion of NR cells in cluster 10. Thus, I saw a correlation of most cytokine production and sensitivity and a positive patient response.

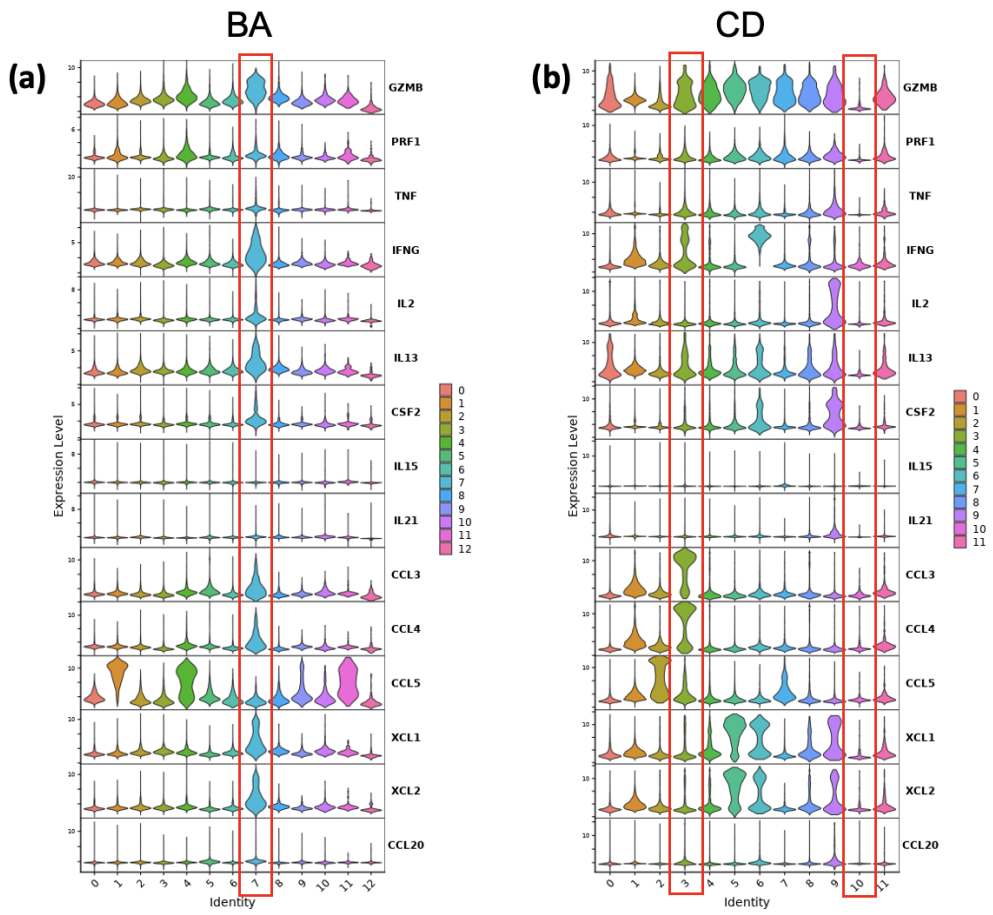

Figure 10: Notable RNA markers through cytokine and other immunological gene expression levels.
(a) Basal state cell subset. Cluster 7 is boxed in red, with a notably higher expression of most labeled genes, including cytotoxic, helper, stimulatory, and chemokine-related T cell markers.
(b) Stimulated cell subset. Clusters 3 and 10 are boxed in red. Cluster 3 show higher expression of chemokine-related activities, while cluster 10 show a lack of expression across all T cell subtype markers.

The results of pathways identified from individual unsupervised clusters were confirmed with the markers defining the 4 main categories of samples: basal state CR/HD, stimulated CR/HD, basal state NR, and stimulated NR (Figure 11). Most notably, the markers of CR/HD cells were much greater in number than markers of NR cells. For GO analysis, the top 500 markers for CR/HD sample subsets were used. Basal state CR/HD cells were involved in regulation of cell migration and cytokine production, while stimulated CR/HD cells worked in immune cell activation, cell migration, and cell motility (Figure 11ab). Both basal state and stimulated NR cells showed very similar activities in protein translation, localization, and ER targeting (Figure 11cd).

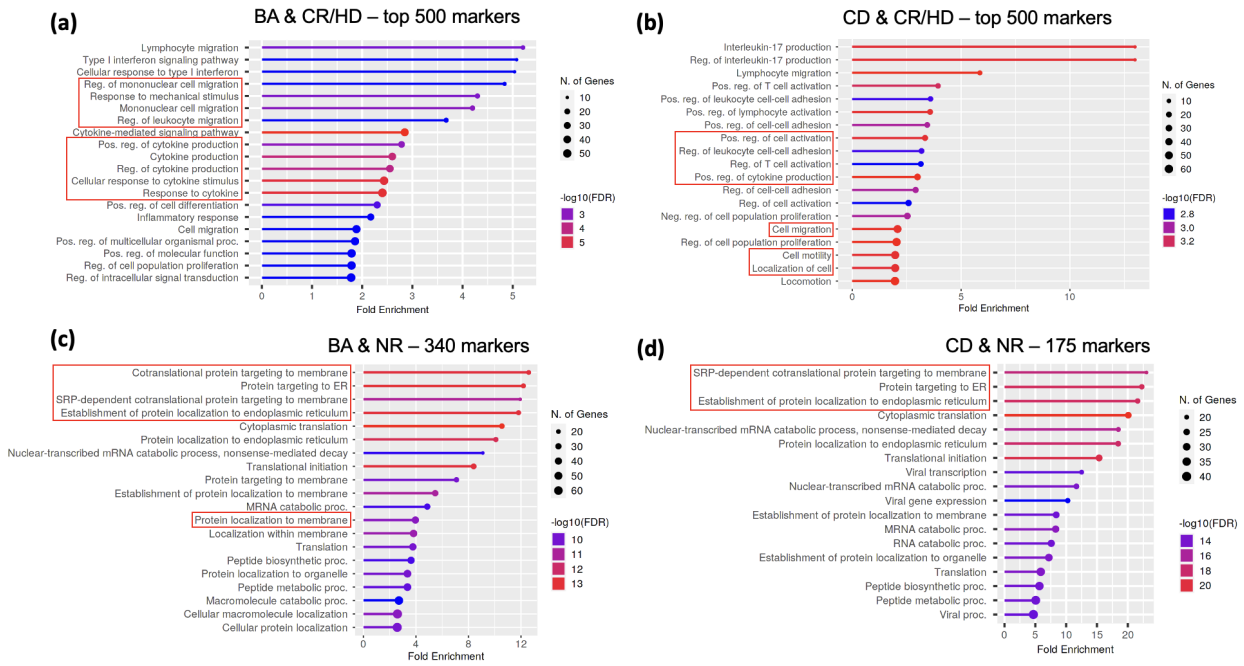

Figure 11: GO analysis of the overall grouping of integrated data.

(a) BA and CR/HD pathways, taken from the top 500 markers of the subset. Boxed in red shows the most recurring pathways noted in the list, including migration, cytokine production, and stimulus responding.

(b) CD and CR/HD pathways, taken from the top 500 markers similar to (a). Most notable pathways include cell activation, cell-cell adhesion, cell migration, motility, and localization.

(c) BA and NR pathways, from all key markers (340) of the subset compared to the rest of the cell dataset. Most notable pathways include protein targeting to ER, protein localization, and translational activities

(d) CD and NR pathways, from 175 markers of the subset. Pathways are similar to (c). CAR T funcion-irrelevant pathways such as viral transcription and viral gene expression are disregarded.

It was uncertain whether the high expression of regulatory pathways and genes on no response cells were due to relatively lower CAR T functions, or whether regulatory activities was truly overexpressed, possibly defining the unactivated NR clusters as Treg cells. One key regulatory gene, *TGFB1*, which produces the protein transforming growth factor beta-1, appeared as a highly differentially expressed marker of BA (Figure 5a) as well as NR cells. When the overall expression between the 3 types of samples (CR/NR/HD) was compared, the expression was markedly higher in NR cells (Figure 12a). The expression levels in the unsupervised clusters of the overall integrated dataset showed a much lower expression in cluster 3, which was also the cluster with the highest CR/HD proportion (Figure 8b). The analysis of *TGFB1* indicated that the absolute expression levels of regulatory genes were indeed higher in NR cells compared to CR/HD cells.

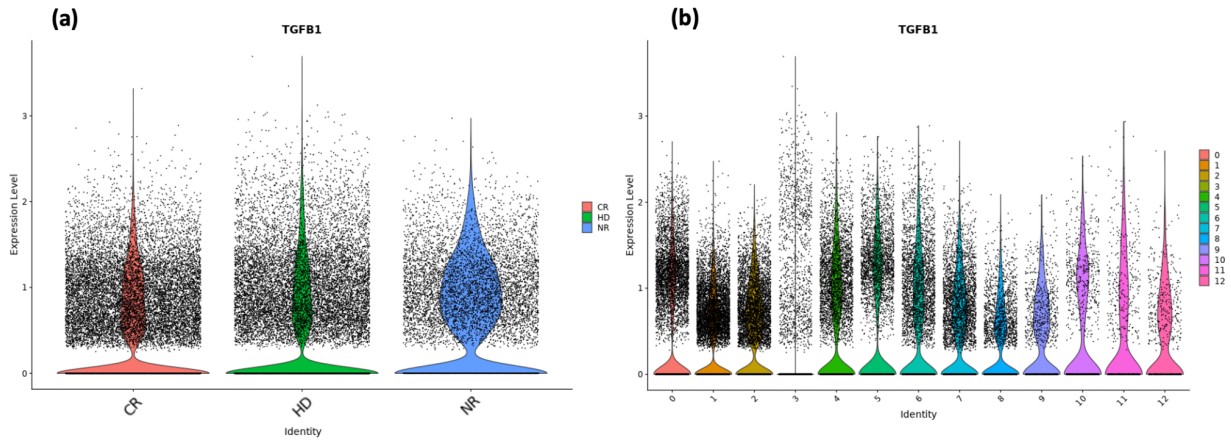

Figure 12: Production of *TGFB1* visualized with overall sample types and unsupervised clusters.
(a) *TGFB1* expression in overall CR (red), HD (green), and NR (blue) populations through a violin plot visualization. Expression levels in NR is significantly higher as evident from the width of the violin.
(b) *TGFB1* expression in the unsupervised clustering of 13 clusters from the overall integrated data. All clusters show an expression level of ~1 count, except for cluster 3, which centers around expression 0.

To confirm the immunological findings and correlate gene expression with expression levels of similar-functioning proteins, ADT analysis was performed on the overall profiles of CR, HD, and NR samples. The Fas apoptotic protein (CD95) as well as CD28, one involved in apoptotic regulation, were both expressed higher in NR cells than CR and HD cells (Figure 13). The CD62L protein, found to be a regulation marker in the HD dataset, was expressed higher on NR cells, while the two activation markers, HLA-DR and CD69, were higher in CR and HD cells. Thus, NR cells had higher apoptotic regulation and would be susceptible to a greater induced cell death, inhibiting proliferation.

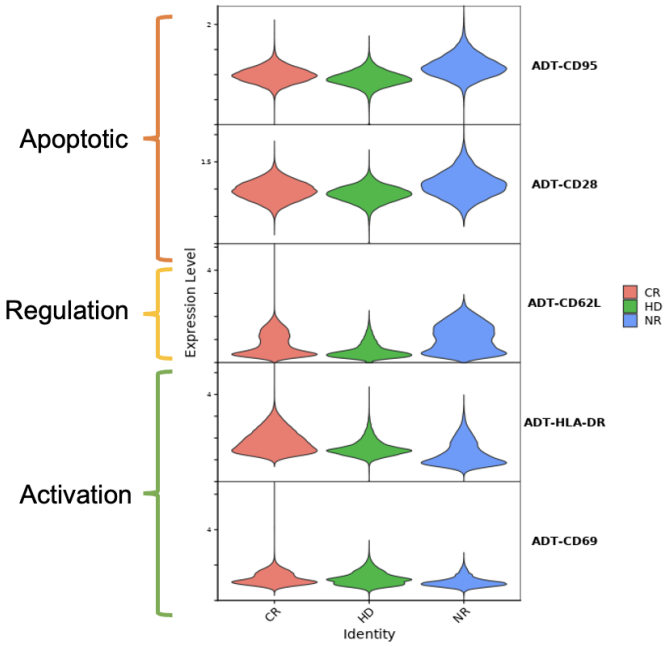

Figure 13: Key ADT markers expressed differentially between CR (red), HD (green), and NR (blue) samples. Apoptotic markers are the CD95 (Fas) and CD28 proteins. The regulation marker CD62L and activation markers HLA-DR and CD69 were derived from the results of the healthy donor dataset analysis, where they marked the differences between BA and CD in HD cells.

DISCUSSION

From the CITE-seq single-cell multiomics data of CAR T cells from healthy donors and no response and complete remission patients, I analyzed the gene expression and comparison between clusters and patient responses to reveal the pathways that distinguished a proper response of a CAR T cell in a tumor microenvironment compared to a malfunctioning one. Even though the CAR engineering was performed uniformly across all donor and patient cells, cells from no response patients were significantly less activated under stimulatory conditions.

From the healthy donor patient data, the similar expression levels of CD4 and CD8 across both the stimulated and the unstimulated subset indicate that either CD4 or CD8 T cells are suitable for becoming CAR T cells that act efficiently for tumor stimulation. This corresponds with several past literature results of CAR T composition and ratios of CD4:CD8 (Lee *et al.* 2018, Turtle *et al.* 2016), and thus confirmed that the healthy donor dataset was working correctly and that the technical workflow is sufficient in analyzing the single cell profiling to come to biologically correct conclusions.

CAR T cells from healthy donor and complete remission patients were found to have significantly different signaling pathways from no response patients. Between CR/HD and NR patients, CD clusters with a high proportion of CR/HD cells showed pathways in known CAR T cells as well as general immunological cell activities such as activation of T cells, leukocytes, and lymphocytes, triggering leukocyte and lymphocyte differentiation, cytokine production and response to cytokine stimuli, and the regulation of various activations and differentiations (Park 2021, Schwab *et al.* 2020). This also involved cell-to-cell adhesion, which suggests that the addition of cell surface proteins contributing to adhesion and enhancing helper functions could be beneficial to overall immunological functions. Furthermore, pathways involving cell motility and migration were increased, suggesting the importance of rapid circulation throughout the body (Simula *et al.* 2022).

Higher cytokine production had a general correlation with better patient response. Cluster 10 of the stimulated subset of integrated HD/CR/NR data, which had a high NR proportion, showed a substantially lower expression of *CCL3, CCL4, CCL5, XCL1, XCL2,* and *CCL20*, notable cytokine-related immunological markers. On the other hand, cluster 7 of the basal state subset had high expression in the first five of those genes and correlated with one of the lowest percentages of NR, the majority being HD cells. Cluster 11 of the basal subset with high expression of *CCL5* in particular had the highest CR proportion and the lowest NR proportion in BA clusters, indicating that *CCL5* could contribute more so than other cytokines to the regulatory state of CAR T cells in patients. Foeng *et al.* showed that the CCL2 and CCL5 cytokines were most common in intratumoral T cell trafficking and tumor infiltration, further confirming these results (Foeng *et al.* 2022). To further confirm the role of cytokines, in the stimulated subsets, the clusters with the lowest NR proportion (1, 3, 5, 6, 9) showed high levels of the 6 cytokine genes compared to other clusters. Most notably, cluster 3 had high levels of *CCL3, CCL4*, and *CCL5*, while clusters 5, 6, and 9 had high levels of *XCL1* and *XCL2*, suggesting the divergence of cytokine production between different subsets of CAR T cells. The differences in HD and CR proportion sizes have yet to be investigated but generally show similar patterns when compared to NR proportions.

One of the most notable characteristics of NR cells was the singular cluster in both the stimulated and basal state subsets that had >75% constituted of NR. This phenomenon can also be observed in the direct comparison of CR to NR patients before the integration of HD cells. Each of these clusters also showed a low expression of most key immunological markers, including *GZMB, PRF1, TNF, IFNG, IL2, IL13, CSF2, XCL1,* and *XCL2*. GO pathways showed no particular activities in immunological activities, and mainly focused on regulatory biological activities such as protein translation and endoplasmic reticulum

activities of protein localization. The activities of the gene TGFB1 were prominent in NR cells, both in general and in subtypes such as cluster 3 of the overall integrated dataset. Blocking the transforming growth factor beta (TGF-β) that comes from *TGFB1* has repeatedly been found to be effective in increasing CAR T cell efficiency against the development of CAR T therapy against solid tumors (Hou *et al.* 2018, Tang *et al.* 2020). The correlation between the reduction in Treg cells and enhanced CAR T cell functions suggests that the subtype of T cells with high proportions of NR cells are a type of Treg cells that proliferate more greatly than the other CAR T subtypes and do not add meaningful activities to therapeutic effects, as they have unchanging activities whether stimulated or not. Knocking out such regulatory and helper genes may not only provide a better efficacy of CAR T cells in B-ALL, but provide a key method to unlocking the potential of CAR T in solid tumors.

The role of proliferation of CAR T cells in patient responses extend further than regulatory subtypes of T cells. In the majority of high CR/HD proportion clusters, GO showed pathways in cell population proliferation, DNA replication, mitotic cell cycle, and cell division activities, indicating that the proliferation activities and thus overall number of CAR T cells contribute greatly to the efficacy of therapy due to their durability and persistence *in vivo*. Clinical results show that T cell subtypes such as central memory (Tcm) and stem-like memory (Tscm) T cells result in a greater outcome of therapy (López-Cantillo *et al.* 2022).

Moreover, NR clusters tended to show higher susceptibility to apoptosis and cell death activities, meaning that the more proliferation is inhibited in CAR T cells, the less likely the patient response is to be positive. The Fas apoptotic protein (CD95) and the apoptotic regulator CD28 were found at a higher expression level on NR than both CR and HD cells. The Fas protein especially, along with other proteins such as FasL, DR5, and TRAIL, results in programmed cell death and are an obstacle to the long-term persistence of CAR T; recombinant Fas proteins have shown to improve CAR T cell apoptosis and CAR activation (Tschumi *et al.* 2018). The role of apoptosis in CAR T cells and how to reduce them in an effective manner to increase CAR T cell survival and proliferation is a further study to be investigated.

CAR T therapy is still undergoing development in its engineering methods and clinical trials, and with the approved methods of therapy through CD19, approximately 10-20% of B-ALl patients have no response and nearly 50% have relapse even without tumor adaptive resistance (Sheykhhasan *et al.* 2022). Because CAR T therapy can provide a cheaper and more accessible alternative than to other forms of immunotherapy and overall cancer treatment, by improving the response rate and effectiveness of CAR engineering, thousands of patients will be able to benefit from high response rate and long-term effects of

CAR T therapy. By identifying characteristics of healthy to malfunctioning CAR T cells, rather than putting the focus on CAR engineering, my analysis will contribute to the further honing and genetic modifications of cellular functions of T cells.

REFERENCES

1. Bai Z, Woodhouse S, Zhao Z, Arya R, Govek K, Kim D, Lundh S, Baysoy A, Sun H, Deng Y, et al. 2022. Single-cell antigen-specific landscape of CAR T infusion product identifies determinants of CD19-positive relapse in patients with ALL. Sci Adv. 8(23):eabj2820.
2. Billingham RE, Brent L, Medawar PB. 1954. Quantitative studies on tissue transplantation immunity. II. The origin, strength and duration of actively and adoptively acquired immunity. Proc R Soc Lond B Biol Sci. 143(910):58–80.
3. Brentjens RJ, Davila ML, Riviere I, Park J, Wang X, Cowell LG, Bartido S, Stefanski J, Taylor C, Olszewska M, et al. 2013. CD19-targeted T cells rapidly induce molecular remissions in adults with chemotherapy-refractory acute lymphoblastic leukemia. Sci Transl Med. 5(177):177ra38.
4. Davila ML, Riviere I, Wang X, Bartido S, Park J, Curran K, Chung SS, Stefanski J, Borquez-Ojeda O, Olszewska M, et al. 2014. Efficacy and toxicity management of 19-28z CAR T cell therapy in B cell acute lymphoblastic leukemia. Sci Transl Med. 6(224):224ra25.
5. Dhatchinamoorthy K, Colbert JD, Rock KL. 2021. Cancer Immune Evasion Through Loss of MHC Class I Antigen Presentation. Frontiers in Immunology. 12.
6. Finn OJ. 2008. Cancer immunology. N Engl J Med. 358(25):2704–2715.
7. Foeng J, Comerford I, McColl SR. 2022. Harnessing the chemokine system to home CAR-T cells into solid tumors. Cell Rep Med. 3(3):100543.
8. Garrido F, Aptsiauri N, Doorduijn EM, Garcia Lora AM, van Hall T. 2016. The urgent need to recover MHC class I in cancers for effective immunotherapy. Curr Opin Immunol. 39:44–51.
9. Grupp SA, Kalos M, Barrett D, Aplenc R, Porter DL, Rheingold SR, Teachey DT, Chew A, Hauck B, Wright JF, et al. 2013. Chimeric antigen receptor-modified T cells for acute lymphoid leukemia. N Engl J Med. 368(16):1509–1518.
10. He Q, Jiang X, Zhou X, Weng J. 2019. Targeting cancers through TCR-peptide/MHC interactions. Journal of Hematology & Oncology. 12(1):139.
11. Hou AJ, Chang ZL, Lorenzini MH, Zah E, Chen YY. 2018. TGF‐β–responsive CAR‐T cells promote anti‐tumor immune function. Bioeng Transl Med. 3(2):75–86.
12. June CH, O'Connor RS, Kawalekar OU, Ghassemi S, Milone MC. 2018. CAR T cell immunotherapy for human cancer. Science. 359(6382):1361–1365.
13. June CH, Sadelain M. 2018. Chimeric Antigen Receptor Therapy. N Engl J Med. 379(1):64–73.
14. June CH, Warshauer JT, Bluestone JA. 2017. Is autoimmunity the Achilles' heel of cancer immunotherapy? Nat Med. 23(5):540–547.

15. Le RQ, Li L, Yuan W, Shord SS, Nie L, Habtemariam BA, Przepiorka D, Farrell AT, Pazdur R. 2018. FDA Approval Summary: Tocilizumab for Treatment of Chimeric Antigen Receptor T Cell Induced Severe or Life Threatening Cytokine Release Syndrome. Oncologist. 23(8):943–947.
16. LeBien TW, Tedder TF. 2008. B lymphocytes: how they develop and function. Blood. 112(5):1570–1580.
17. Lee DH, Cervantes-Contreras F, Lee SY, Green DJ, Till BG. 2018. Improved Expansion and Function of CAR T Cell Products from Cultures Initiated at Defined CD4:CD8 Ratios. Blood. 132(Supplement 1):3334.
18. Lee DW, Gardner R, Porter DL, Louis CU, Ahmed N, Jensen M, Grupp SA, Mackall CL. 2014. Current concepts in the diagnosis and management of cytokine release syndrome. Blood. 124(2):188–195.
19. Lin X, Lee S, Sharma P, George B, Scott J. 2022. Summary of US Food and Drug Administration Chimeric Antigen Receptor (CAR) T-Cell Biologics License Application Approvals From a Statistical Perspective. JCO. 40(30):3501–3509.
20. López-Cantillo G, Urueña C, Camacho BA, Ramírez-Segura C. 2022. CAR-T Cell Performance: How to Improve Their Persistence? Frontiers in Immunology. 13.
21. Mitchison NA. 1955. Studies on the immunological response to foreign tumor transplants in the mouse. I. The role of lymph node cells in conferring immunity by adoptive transfer. J Exp Med. 102(2):157–177.
22. Park CH. 2021. Making Potent CAR T Cells Using Genetic Engineering and Synergistic Agents. Cancers (Basel). 13(13):3236.
23. Schwab RD, Bedoya DM, King TR, Levine BL, Posey AD. 2020. Approaches of T Cell Activation and Differentiation for CAR-T Cell Therapies. Methods Mol Biol. 2086:203–211.
24. Sengsayadeth S, Savani BN, Oluwole O, Dholaria B. 2021. Overview of approved CAR‐T therapies, ongoing clinical trials, and its impact on clinical practice. EJHaem. 3(Suppl 1):6–10.
25. Sheykhhasan M, Manoochehri H, Dama P. 2022. Use of CAR T-cell for acute lymphoblastic leukemia (ALL) treatment: a review study. Cancer Gene Ther. 29(8):1080–1096.
26. Simula L, Ollivier E, Icard P, Donnadieu E. 2022. Immune Checkpoint Proteins, Metabolism and Adhesion Molecules: Overlooked Determinants of CAR T-Cell Migration? Cells. 11(11):1854.
27. Tang N, Cheng C, Zhang X, Qiao M, Li N, Mu W, Wei X-F, Han W, Wang H. 2020. TGF-β inhibition via CRISPR promotes the long-term efficacy of CAR T cells against solid tumors. JCI Insight. 5(4).
28. Teachey DT, Lacey SF, Shaw PA, Melenhorst JJ, Maude SL, Frey N, Pequignot E, Gonzalez VE, Chen F, Finklestein J, et al. 2016. Identification of Predictive Biomarkers for Cytokine Release

Syndrome after Chimeric Antigen Receptor T-cell Therapy for Acute Lymphoblastic Leukemia. Cancer Discov. 6(6):664–679.

29. Torikai H, Reik A, Liu P-Q, Zhou Y, Zhang L, Maiti S, Huls H, Miller JC, Kebriaei P, Rabinovitch B, et al. 2012. A foundation for universal T-cell based immunotherapy: T cells engineered to express a CD19-specific chimeric-antigen-receptor and eliminate expression of endogenous TCR. Blood. 119(24):5697–5705.
30. Tschumi BO, Dumauthioz N, Marti B, Zhang L, Schneider P, Mach J-P, Romero P, Donda A. 2018. CART cells are prone to Fas- and DR5-mediated cell death. j immunotherapy cancer. 6(1):71.
31. Turtle CJ, Hanafi L-A, Berger C, Gooley TA, Cherian S, Hudecek M, Sommermeyer D, Melville K, Pender B, Budiarto TM, et al. 2016. CD19 CAR–T cells of defined CD4+:CD8+ composition in adult B cell ALL patients. J Clin Invest. 126(6):2123–2138.
32. Wang Z, Cao YJ. 2020. Adoptive Cell Therapy Targeting Neoantigens: A Frontier for Cancer Research. Frontiers in Immunology. 11.
33. Zakrzewski JL, Suh D, Markley JC, Smith OM, King C, Goldberg GL, Jenq R, Holland AM, Grubin J, Cabrera-Perez J, et al. 2008. Tumor immunotherapy across MHC barriers using allogeneic T-cell precursors. Nat Biotechnol. 26(4):453–461.
34. Zhang C, Liu J, Zhong JF, Zhang X. 2017. Engineering CAR-T cells. Biomark Res. 5:22.